Available online at www.sciencedirect.com

ScienceDirect

Defence Technology 10 (2014) 119–123

www.elsevier.com/locate/dt

Formation of explosively formed penetrator with fins and its flight characteristics

Jian-qing LIU*, Wen-bin GU, Ming LU, Hao-ming XU, Shuang-zhang WU

College of Field Engineering, PLA University of Science & Technology, Nanjing 210007, China

Received 18 February 2014; revised 8 April 2014; accepted 6 May 2014
Available online 20 May 2014

Abstract

The ultimate goal of weapon system employing an explosively formed penetrator (EFP) is to defeat a target at the longest standoff. In order to do this, an EFP must be aerodynamically stable so as to strike the target at a small angle of obliquity, and the decay velocity per meter of EFP must be smaller at extended standoff. As the angle of attack increases, the penetration ability of EFP greatly reduces. The fins improve the EFP aeroballistic characteristics and decrease the flight drag of EFP as well. EFP with fins formed by three-point initiation is presented. The formation of EFP with fins is studied by LS-DYNA, and the aeroballistics is studied through experiment. The experimental results show that the decay velocity per meter of EFP with fins is much smaller than that of normal EFP, and the attitude angle steadily decreases.

Keywords: EFP with fins; Multi-point initiation; Flight characteristics

1. Introduction

Explosively formed penetrators (EFPs) have been used in a number of munition systems to defeat armor, masonry and concrete targets. EFPs are launched from considerable distance from their targets. In order to do this, EFPs must be aerodynamically stable so as to strike the target with a small angle of obliquity , and the decay velocity per meter of EFP must be smaller. In recent years, a great deal of effort focused on optimizing the liner, shaper, and initiation process for EFPs which possess desirable aerodynamic and penetration characteristics [1–3]. Abundant research results indicate that forming EFP with fins improves its aerodynamic stability and hit accuracy [2,4]. Experimental and numerical results show that multi-point initiation is a simple and feasible technique for forming EFPs with fins.

In this paper, EFP with fins formed by three-point initiation was designed to study the whole process of its formation and flying characteristics. The formation process of EFP with fins was analyzed by LS-DYNA and the aeroballistic study was conducted through experiment.

2. EFP warhead configuration

EFP warhead consists of synchronous three-point explosive circuit and main charge, as shown in Fig. 1.

2.1. Main charge

High explosive JH-2 is used as main charge. The density, length and diameter of charge are 1.7 g/cm^3, 32.5 mm and 65 mm, respectively. The liner is made of copper, and the configuration of liner with variable wall-thickness is hemispherical. The exterior and interior surface curvatures of liner

* Corresponding author.
E-mail address: qq5893736@163.com (J.Q. LIU).
Peer review under responsibility of China Ordnance Society.

Production and hosting by Elsevier

http://dx.doi.org/10.1016/j.dt.2014.05.002

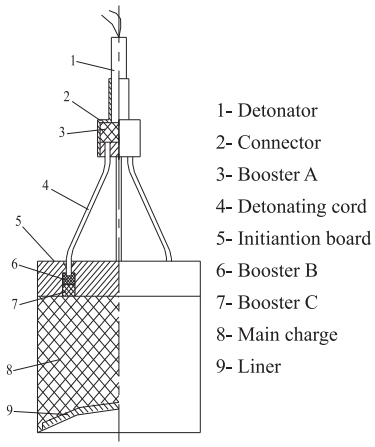

Fig. 1. Warhead configuration.

are 70 mm and 78 mm, respectively. The thickness of liner at vertex is 2.8 mm. Numerical simulation indicates that hemispherical liner with variable wall-thickness is benefit of forming EFP with more appropriate configuration.

2.2. Synchronous three-point explosive circuit

The synchronous three-point explosive circuit (Fig. 2) controls the detonation wave configuration of shaped charge. An "One In Three Out" explosive circuit was designed (Fig. 2). It consists of detonating cord, initiation board, booster A, B and C. Initiation capacity and synchronization of three-point explosive circuit are critical to wave control. In an attempt to improve the initiation capacity and synchronization, the initiation sequence was optimized. The parameters of initiation sequence are listed in Table 1.

The synchronization and initiation capacity of explosive circuit were measured (see Fig. 3). The synchronization of three point detonation wave output was measured by probes, the initiation capacity was measured by the witness copper plate which was placed under the explosive circuit. Three tests in one of which the data was not captured were conducted. The experimental results of the three-point synchronous explosive circuit are shown in Table 2. The error of initiation time (Δt) was smaller than 0.3 μs. The EFP forming experiments indicate that the synchronization of three-point explosive circuit is feasible. Three dints were produced on each of the witness copper plate by the outputs of initiation points (see Fig. 4).

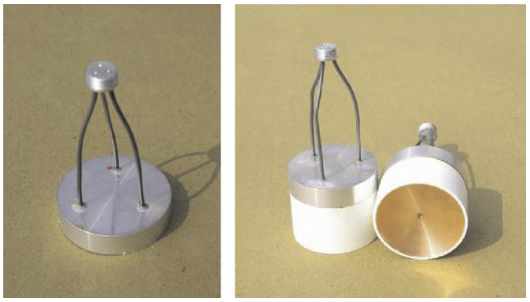

Fig. 2. Synchronous three-point explosive circuit.

Table 1
The parameters of initiation sequence.

Component	Explosive	Diameter/mm	Length/mm	Density ($g \cdot cm^{-3}$)
Booster A	Passivated RDX	15.0	6.7	1.58
Detonating cord	–	2.4	125.0	1.29
Booster B	RDX	5.0	5.0	1.48
Booster C	RDX	5.0	5.0	1.60

The holes on initiation board in which the booster B and C were filled were enlarged by detonation products (see Fig. 4).

The test results of witness copper plates and detonation initiation boards are shown in Table 3, where H_c is the depth of dint on the witness copper plate, and D_h is the diameter of hole on initiation board. The values of H_c are between 2.86 mm and 3.46 mm, and its average value is 3.11 mm. The diameter of original hole on initiation board is 5 mm. After tests, the values of D_h are between 8.04 mm and 9.74 mm, and its average value is 9.06 mm. The results indicate that the outputs of initiation points are reliable, and the design of explosive circuit is reasonable.

3. Numerical simulation of EFP forming process

The computational model of EFP warhead is shown in Fig. 5. EFP forming process was simulated by LS-DYNA. The copper liner was deformed by the detonation wave and products. Fig. 6 shows the outlines of EFP at different time instants. In general, the axial velocities of liner top elements are faster than those of the bottom elements, forming a turning backward mode like the conventional EFPs with coned or flared tails. At the same time, the main charge was initiated by

Fig. 3. The synchronization and initiation of explosive circuit test setup.

Table 2
The experimental results of three-point synchronous explosive circuit.

Test	Initiation time of initiation point/μs			Δt/μs
	1	2	3	
1	21.2	21.1	21.4	≤0.3
2	21.1	20.9	21.2	≤0.3

Witness copper plates

Detonation transmitting boards

Detonation transmitting boards

Fig. 4. Witness copper plates and initiation boards test results.

Table 3
The test results of three-point synchronous explosive circuit.

Initiation points	Test 1			Test 2			Test 3		
	1	2	3	1	2	3	1	2	3
H_c/mm	3.44	3.46	2.86	3.06	3.24	2.98	2.98	3.54	3.46
D_h/mm	8.76	9.20	8.74	9.10	9.44	8.04	9.42	9.74	–

the three-point explosive circuit, producing three spherical detonation waves that interacted with each other. Therefore, the forebody of EFP was not cylindrical in shape, and three fins were formed in the tail of EFP. The fins were situated on the symmetry surface between two of the initiation points. The number of fins is equal to the number of initiation points.

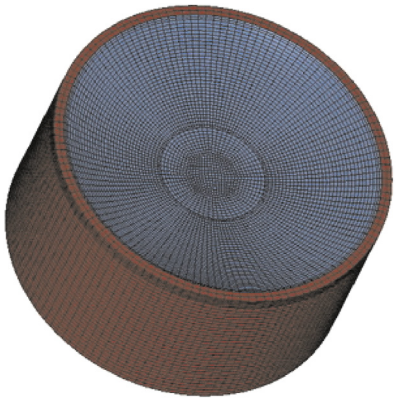

Fig. 5. Numerical modeling of EFP warhead.

4. Full size warhead test

4.1. Test setup

Fig. 7 shows the test setup for the forming and aeroballistic characteristics of EFP. Three EFP warheads discussed above were fired. As EFPs flew downrange after formation, the data which represents their exterior shape, velocity and flight performance was collected. The dropping velocity as a function of standoff was obtained using eight silver paper bars placed along the flight path interval of 5 m from 5 m to 40 m; and six yaw paper screens were plastered with silver paper bars placed from 5 m to 30 m. After each yaw screen is in place, the horizontal and vertical cross-hairs are painted upon it at a known location, enabling the EFP flight path to be determined as it flies downrange. The precise time of EFP perforating each silver paper bar is recorded so that the velocity of EFP (V_e) at different standoff is calculated by the elapsed time.

4.2. Velocity and shape of EFP

The test data indicate that the dropping velocities (V_e) of EFPs with fins are consistent from shot to shot. Table 4 lists the test results of V_e, average V_e and velocity decay per meter of EFPs at different ranges. The former experimental research indicates that the velocity decay per meter of conventional EFPs with coned or flared tails is about 27.3 m/s. Therefore, the fins could decrease the flight drag of EFP observably.

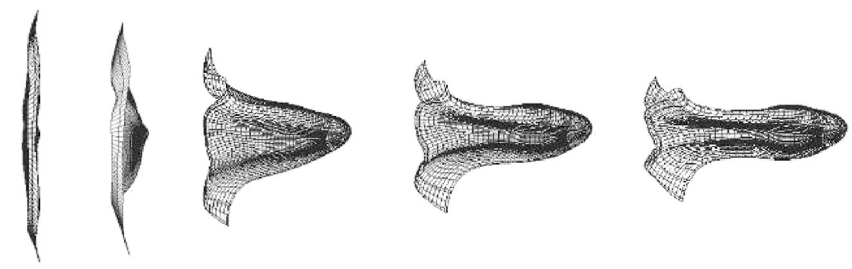

Fig. 6. Simulated results of EFP with fins forming process.

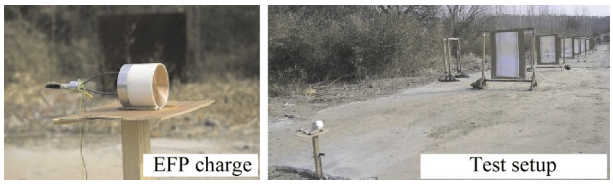

Fig. 7. Full size warhead test setup.

Table 4
The experimental results of the velocities of EFPs with fins.

Test	Range/m	7.5	12.5	17.5	22.5	27.5
1	V_e/(m·s^{-1})	1731	1663	1612	1548	1470
2		1699	1651	1623	1514	1444
3		–	1611	1601	1541	1471
Average V_e/(m.s^{-1})		1715	1642	1612	1534	1462
Velocity decay/(m.s^{-1})		12.6	6.0	15.6	14.5	

The detailed shape of EFP with fins obtained by numerical simulation is shown in Fig. 8. A great deal of information could be obtained by examining the yaw screens. While the yaw screens can not be used to completely define EFP shape, they are extremely useful in estimating the forebody and fin shape except the length of EFP. Because of the length of EFP captured by yaw screen is determined by the angle of attack, which is normally smaller than the real length of EFP. The information about the shapes of fins can be generated on the screen at a low angle of attack, and the information about the whole shape of EFP body can be generated on the screen at a large angle of attack (See Fig. 9).

Table 5 shows the numerical simulation and test results of EFP shape and initial velocity. In Table 5, V_i is the initial velocity, D is the largest diameter of forebody, L is the length, and D_w is the wingspan. All of the test data are the average value except the value of L in Table 5. The value of L is the length of the largest hole on the yaw screen. An initial velocity of EFP is 1766 m/s, $L/D = 1.8$, and $D_w/D = 1.3$.

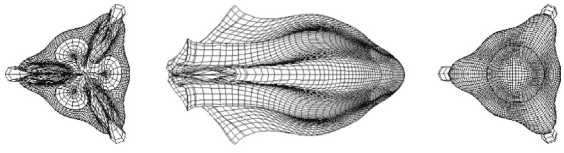

Fig. 8. Numerical simulation result of EFP shape.

Table 5
The numerical and test results of EFP forming characteristics.

	V_i/(m·s^{-1})	D/mm	L/mm	D_w/mm
Test	1766	26.1	46.8	33.4
Simulation	1715	26.5	>40.0	35.8

4.3. Angle of attack

The more important information obtained from the yaw screens (See Fig. 10) is perhaps the roll and angle of attack data. The roll of EFP is the result of unintentional asymmetry, most likely in the tail region, generated by formation process. It is difficult to estimate the accurate roll rate of EFP.

But, for EFPs with fins which were not designed to have any zero spin roll torque, the roll torque values perhaps randomly vary from shot to shot. This variable roll behavior is undesirable since a repeatable roll rate is necessary to guarantee dynamic stability [4]. The explosive formation process induces the significant initial disturbances to EFP. So it is unavoidable that the EFPs have thr initial angles of attack and the angles vary from shot to shot.

The length of EFP captured by yaw screen is a function of the angle of attack. The data in Table 5 indicates that the numerical and experimental results are very consistent. Therefore, The value of "L" obtained by numerical simulation can be taken as the real length of EFP. The angles of attack were estimated, as shown in Fig. 11. The initial angles of attack are 20–35°. As the EFPs fly downrange, their angles of attack vary dramatically. For two of EFPs, Shots 1 and 3, their largest angles of attack experienced a decrease as they flew downrange. For Shot 3, the largest angle of attack varied slightly. All of the shots experienced the increase in the angle of attack rates as they flew downrange. Based on the test result, the aerodynamic stability of EFP is enhanced due to stabilization moment by fins so as to strike the target with a small angle of attack.

5. Conclusions

Computer simulations and test results shown that an EFP with fins can be formed by the designed three-point explosive circuit. The fins decrease the flight drag of EFP observably over conventional EFPs with coned or flared tails and improve the aerodynamic stability of EFP so as to enhance the ability of defeating target.

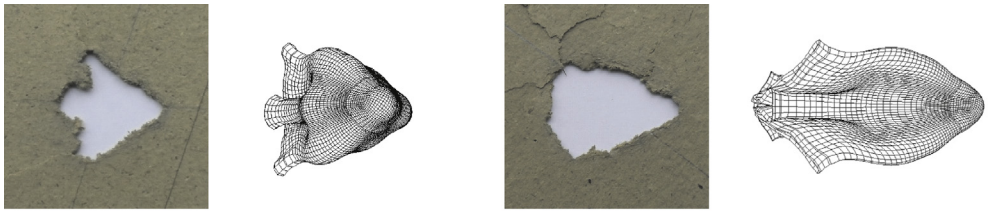

Fig. 9. Shapes of EFPs with fins at different angles of attack.

Shot 1 Shot 2 Shot 3

Fig. 10. Yew screens of full range.

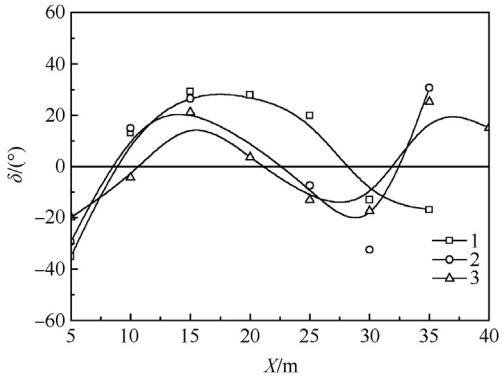

Fig. 11. Angle of attack vs. flying range.

References

[1] Bouet TH, Tarayre P, Guillon JP. Study of a multi-point ignition EFP. In: 15th International Symposium on Ballistics. Israel; 1995. pp. 159−66.

[2] Bender D, Chhouk B, Fong R, Rice B, Volkmann E. Explosively formed penetrators (EFP) with canted fins. In: 19th International Symposium on Ballistics. Switzerland; 2001. pp. 755−61.

[3] Yu C, Dong QD, Sun CW, Tong YJ, Yan CL, Li FB, et al. The experimental studies of explosively formed projectile with star shaped tail. Explos Shock Waves 2003;23(6):561−4.

[4] Malejko G, Grau J. Flight performance of an explosively formed penetrator. In: 31st Areospace Sciences Meeting & Exhibit, Renn, NV; 1993.